Development of freeze-dried kit for the preparation of [^{99m}Tc]Tc-HYNIC-ALUG: A potential agent for imaging of prostate specific membrane antigen

Tanveer Hussain Bokhari[1,†], Fehmida Bibi[1,†], Muhammad Irfan[2], Faiz Ahmed[1], Talal Abdul Rahman[3], Shazia Fatima[3], Muhammad Zeeshan[1], Maria Hassan[1], Adam Safi Ullah[1], Muhammad Wasim[2], Nadeem Ahmed Lodhi[2]

[1]Department of Chemistry, Government College University, Faisalabad, Pakistan
[2]Isotope Production Division, Pakistan Institute of Nuclear Science and Technology, Nilore, Islamabad, Pakistan
[3]Karachi Institute of Radiotherapy and Nuclear Medicine, Karachi, Pakistan

[†]These authors contributed equally.

Corresponding author:
Dr. Nadeem Ahmed Lodhi
Isotope Production Division, Pakistan Institute of Nuclear Science & Technology (PINSTECH), Nilore, Islamabad
E-mail: nadeem007@snu.ac.kr

Running title: Preparation and clinical evaluation of [^{99m}Tc]Tc-HYNIC-ALUG

Article History:
Received: 08 October 2023
Revised: 29 January 2024
Accepted: 31 January 2024
Published Online: 25 March 2024

ABSTRACT

Introduction: Prostate-specific membrane antigen (PSMA) is increasingly recognized as a viable target for imaging and therapy of Prostate cancer (PCa). In this study, we introduce the freeze-dried kit formulation of [^{99m}Tc]Tc-HYNICALUG for easy clinical evaluation of prostate cancer.

Methods: In this work, an in silico modeling of the urea-based PSMA small molecule (HYNIC-ALUG) was performed to check its interaction with human glutamate carboxypeptidase II and compared it with experimental results. The HYNIC-PSMA kit was formulated for easy preparation of [^{99m}Tc]Tc-HYNIC-ALUG. The kit contained a freeze-dried mixture of HYNIC-ALUG, coligands $SnCl_2.2H_2O$, and antioxidant D-mannitol.

Results: The calculated Ki value (inhibition/dissociation constant) was 4.55 which showed excellent binding affinity of HYNIC-ALUG with PSMA. miLogP and cLogS values are -4.04 and -3.07 respectively showing its hydrophilic character and predicting its excellent distribution in biological fluids. Subsequently, the radiochemical purity of the HYNIC-PSMA kit was 99.1 ± 1.32% (n = 6) determined by radio-ITLC and by HPLC as well. In vitro stability in saline and serum was studied up to 4 h and showed high stability (≥ 96%). The distribution of [^{99m}Tc]Tc-HYNIC-ALUG was carried out in two patients and SPECT/CT planar images were acquired at 2h

and 4h respectively. Bio-physiological distribution of [^{99m}Tc]Tc-HYNIC-ALUG was observed normally in lacrimal, salivary glands, liver, spleen, gut, kidneys, and urinary bladder.
Conclusion: The HYNIC-ALUG freeze-dried kit could be used for easy preparation of [^{99m}Tc]Tc-HYNIC-ALUG and can be considered as a potential agent for the diagnosis, staging, and restaging of advanced prostate cancer.

Keywords: Prostate cancer; Technetium-99m; HYNIC-ALUG; SPECT imaging; Clinical evaluation

INTRODUCTION

Prostate cancer is the most prevalent kind of malignancy in males all over the world. In 2022 the expected number of new cases of prostate cancer in the United States was 268,490. Approximate mortality rate from prostate cancer is 34,500 [1, 2]. In the case of localized disease, surgery and radiotherapy are the primary treatments [3]. While, in recurring or metastatic disease, androgen signaling inhibition (ARSI), androgen-deprivation therapy (ADT), and chemotherapy are the primary medical treatments [4]. However, most individuals develop castration resistance, which correlates with an adverse prognosis. Prostate-specific antigen (PSA) assay is a commonly employed diagnostic approach in Prostate cancer patients; whereas, this investigation cannot identify tumors or differentiate between PCa stages to determine suitable therapy [5].

PSMA, or prostate-specific membrane antigen (PSMA), is an enzyme that appears in prostate epithelial cells and is identified in 95% of advanced prostate cancers (PCa). The majority of prostate cancers express PSMA making it an effective biomarker for targeted radionuclide treatment and clinical assessment [6]. Expression levels of PSMA are directly associated with metastasis, development of PCa, and androgen independence [7, 8]. As a result, PSMA is a first-rate molecular goal for imaging as well as the therapy of advanced prostate cancer with particular radiopharmaceuticals [9]. PSMA expression is elevated in undifferentiated metastatic tumors at the hormone-sensitive and castration-resistant stages, suggesting that it could be used as an early progression marker [10]. Furthermore, higher PSMA expression in prostate cancer relates with other undesirable diagnostic indicators and predicts many adverse outcomes independently. Its expression rises gradually with metastatic castration-resistant prostate cancer (mCRPCa) and advanced PCa. Therefore PSMA appears to be an outstanding candidate for development of theranostic radiopharmaceuticals for prostate cancer [11].

Flourine-18 (^{18}F) Positron Emission Tomography (PET) based PSMA radiotracers [^{18}F]JK-PSMA-7, [^{18}F]AlF-PSMA-11 and [^{18}F]PSMA-1007 [12] have been clinically established radiopharmaceuticals. However, due to the requirement of costly installation and maintenance of cyclotron, time-consuming and challenging radiosynthesis and short half-life of ^{18}F (110 min) poses some challenges in the preparation as compared to ^{68}Ga-based radiopharmaceuticals [13, 14]. Despite the success of [^{68}Ga]Ga-PSMA in imaging prostate cancer, there are obstacles in providing the growing requirement for this imaging modality in the treatment of patients. In a single elution, the amount of ^{68}Ga obtained from the 68Ge/68Ga generator is adequate to synthesize radiotracer for some patients only. Consequently, number of patients who can be diagnosed in one day is limited [15]. Moreover, currently, a few PET cameras have been placed globally than the majority of other diagnostic instruments, that restricts the importance of this utility in daily medical treatment [15].

^{99m}Tc decays by emitting 140 keV -rays (89% abundance) and it is appropriate for single photon emission computerized tomography (SPECT) imaging as well as can deliver low-radiation doses

to patients [16]. Furthermore, its $t_{1/2}$ 6-h (half-life) is adequate for ^{99m}Tc radiopharmaceutical preparation in hospitals and makes it possible for their quality control, administration to patients, and accumulation in the targeted organ as well as image acquisition [17]. Moreover, the ^{99}Mo/^{99m}Tc generator is an easy way to get ^{99m}Tc and it is primary reasons that ^{99m}Tc has become one of the most extensively utilized radionuclides in the field of nuclear imaging [18, 19]. [^{99m}Tc]Tc-PSMA radiotracers currently being used are [^{99m}Tc]Tc-MAS$_3$-y-nal-k(Sub-KuE) [20] , [^{99m}Tc]Tc-GRFLT-ECG-ROX [21], [^{99m}Tc]Tc-MIP-1427 [21, 22], [^{99m}Tc]Tc-PSMA I&S [21] and [^{99m}Tc]Tc-MIP-1405 [23]. [^{99m}Tc]Tc-HYNIC-ALUG is a small molecular inhibitor without lipophilic linkers reported by Xiaoping and showed promising results in identification of PCa [11]. In this research, computational In silico simulations were conducted to investigate the interaction between [^{99m}Tc]Tc-HYNIC-ALUG and PSMA. Subsequently, a HYNC-ALUG kit was developed to prepare the [^{99m}Tc]Tc-HYNIC-ALUG for the identification of PCa. This kit enables strong and high-yield ^{99m}Tc-labeling by employing easy and common one-step process. The kit comprises a precursor (lyophilized mixture), coligands, buffers as well, and antioxidants, which enhance the stability of the product. Additionally, a clinical evaluation of the [^{99m}Tc]Tc-HYNIC-ALUG was performed on patients with the approval of the ethical review committee.

MOTHODS

Materials

All chemicals were obtained from commercial sources and used without any further purification. Tricine (N- [Tris (hydroxymethyl)methyl] glycine), D-mannitol, stannous chloride ($SnCl_2.2H_2O$) and HCl were purchased from Sigma Aldrich. Monobasic dihydrogen sodium phosphate (NaH_2PO_4), dibasic disodium biphosphate ($Na_2HPO_4.2H_2O$), acetonitrile, butanone ($CH_3CH_2COCH_3$) and trisodium citrate was purchased from Merck KGaA, Germany. Ethylenediamine-N, N′-diacetic acid (EDDA) was purchased from Tokyo Chemical Industry Co Ltd. Japan. PSMA peptide HYNIC-ALUG was purchased from CASLO Aps, Denmark. Na[$^{99m}TcO_4$]$^-$ elution was obtained from ^{99}Mo/^{99m}Tc PAKGEN generator manufactured indigenously by the Isotope Production Division, Pakistan Institute of Nuclear Science and Technology (PINSTECH). Thin layer chromatography was performed on ITLC-SG paper (Agilent Technologies USA). Radio-TLC was counted using a Mini-Scan (Eckert & Ziegler, Germany) system imaging scanner. The activity was measured using a dose calibrator (CAPINTECH, USA Inc.). SPECT-CT gamma camera GE870NM, was used for planar imaging and topographic localization. Dual-head SPECT acquisition included 64 projections, 25 s/projection, matrix 256 × 256. CT scan was performed in the helical mode. Acquisition parameters included settings at 130 kV, 30 mA: 3–5 mm slice thickness. Any focal abnormal uptake of [^{99m}Tc]Tc-HYNIC-ALUG above the surrounding background level, not associated with physiological biodistribution was reported as malignancy.

Statistical analysis

All experiments were performed for thrice and quantitative data was expressed as mean ± SD. P values <0.05 were taken to express a significant difference. Results are provided as mean ± SD. The results of physiological distribution are presented as a percentage of the dose administered per gram of tissue (%ID g^{-1}) as average value with standard deviation (%ID g^{-1}; mean ± standard deviation (SD)) with n representing the number of animals per group.

Molecular docking

AutoDockTools 4.2.6 version 1.5.6 (ADT) was used for molecular modeling using AutoGridTools to calculate the grid array for the ligand interaction on the receptor molecule with an area of 71 x 71 x 71 and several points to be marked by spacing of 0.375 ºA with grid center 17.624, 49.742, 45.124 x, y and z dimensions around the active pocket respectively.

Quantitative structure-activity relationship (QSAR) of PSMA

PSMA QSAR calculations performed with OSIRIS Data Warrior version 5.5.0 and Molinspiration Property Calculation Service (Molinspiration Cheminformatics, n.d.) to calculate toxicity risk and various molecular parameters. Hartree was computed using RB3LYP computation method together with basis set 6-31+G(d,p) through Gaussian 16 and GaussView 6 tools.

Formulation of HYNIC-ALUG Kit

The preparation of the kit was carried out in a clean room facility. For batch preparation of HYNIC-ALUG kit (20 vials per batch), a solution of EDDA (200 mg), tricine (400 mg) and D-mannitol (1 g) was prepared by dissolving in phosphate buffer (15mL, 0.2 M, pH 7.3). HYNIC-ALUG (400 µg/400 µL) and $SnCl_2.2H_2O$ (1 mg/ 1mL, 2 mg) was subsequently added following (20 µg/20 µL) for each vial. Finally, total volume of the solution was adjusted to 20 mL by adding phosphate buffer and final pH was 6.3. The solution (1 mL) was aseptically dispensed to each sterile vial after passing through 0.22 µm Millipore® syringe filter so that each vial contains EDDA (10 mg), tricine (20 mg), D-mannitol (50 mg), HYNIC-ALUG (20 µg) and $SnCl_2.2H_2O$ (100 µg). The vials were lyophilized for 24 h in freeze dryer (freezing at -40 ℃ for 6 h, primary drying for 12 h and secondary drying at 0 ℃ for 2 h and 20 ℃ for 4 h). After freeze-drying the vials were sealed under vacuum and stored at -20 ℃ for further studies.

Kit radiolabeling with Technetium-99m

The preparation of [^{99m}Tc]Tc-HYNIC-ALUG was performed by adding freshly eluted Na[$^{99m}TcO_4$] (1 mL, 7.4 $\times 10^4$ Bq - 1.11$\times 10^9$ Bq) to kit vial and vortexed for 30 second to mix the content of vial and incubated for 15–20 min in boiling water bath. The vial was cooled to room temperature and quality control was performed using ITLC-SG

Quality control

Instant thin layer chromatography impregnated with silica gel (ITLC-SG) was used to analyze radiochemical purity. An Aliquot of sample (2 µL) was drawn from the vial and spotted on ITLC-SG (10 × 2 cm) and developed with methyl ethyl ketone (MEK) and 0.1 M sodium citrate. ITLC developed in MEK, [^{99m}Tc]Tc-HYNIC-ALUG and ^{99m}Tc-colloid remained at origin (Rf = 0-0.1) and free Na[$^{99m}TcO_4$] moved with solvent front (Rf = 0.9-1). Whereas ITLC-SG developed in 0.1 M sodium citrate [^{99m}Tc]Tc-HYNIC-ALUG and free ^{99m}Tc moved with the solvent front (Rf = 0) and ^{99m}Tc-colloids remained at the point of origin (Rf = 0-0.1). A well-type NaI(Tl) detector was used to determine the radioactivity associated with each segment. In contrast, HPLC was performed using gradient elution with water (A) and acetonitrile (B) mixed with 0.1% trifluoroacetic acid as the mobile phase (0-5 min 90% A, 5-15 min 90% A to 10% A, 15-20 min 10% A, 20-25 min 10% A to 90% A, 25-30 min 90% A). Radio-HPLC analysis also showed that there was no obvious decomposition product, which means that the complex had excellent stability in vitro. All 6 batches met the requirements for quality control tests such as appearance, pH,

radiochemical purity, sterility, and apyrogenicity**.** According to the established procedures outlined in the Pakistan pharmacopoeia, the kits passed the tests for apyrogenicity and sterility.

Evaluation of sterility

For the purpose to ensure that the product is safe for human injection, the kit was tested for sterility and bacterial endotoxin test (BET) in accordance with the Pakistan pharmacopeia [World health organization, (2002)]. Sterility test was carried out by dissolving kit components in sterile saline (1mL) and incubating the sample in soyabean casein digest medium (SCDM) at 22.5± 2.5℃ for 14 days to check fungal growth. For testing any bacterial growth, the reconstituted kit was transferred to fluid thioglycolate medium (FTM) and was incubated at 32.5 ± 2.5℃ for 14 days.

Stability studies

The stability of [^{99m}Tc]Tc-HYNIC-ALUG was tested in saline and human serum up to 4 h. [^{99m}Tc]Tc-HYNIC-ALUG (500 µL, 3.7×10^8 Bq) was incubated with human serum (500 µL) for 4h at 37 ℃. After 1, 2, 3 and 4 h respectively, an aliquot of samples (50 µL) was removed from the mixture and methanol (200 µL), centrifuged (12,000 rpm) and spotted on ITLC-SG to check radiochemical purity using method mentioned in quality control section.

Partition coefficient (log P)

The distribution coefficients (Log P) of the [^{99m}Tc]Tc-HYNIC-ALUG was determined by measuring the activity that partitioned between 1-octanol and PBS (pH 7.4) under equilibrium conditions. In brief, octanol (1mL) was added to the [^{99m}Tc]Tc-HYNIC-ALUG (1 mL, 0.2 M Phosphate buffer, pH 7.3, 7.4×10^4 Bq) and vortexed for 5 min. The mixture was allowed to stay for 5 min and centrifuged to separate the two layers. Aliquots (50 µL) were taken from both layers and counts were measured by γ-counter. The log P was calculated using the following equation.

$$\text{Log P} = \text{Log}\ \frac{(\text{cpm in octanol} - \text{cpm in background})}{(\text{cpm in buffer} - \text{cpm in background})}$$

Biodistribution studies

Biodistribution was performed in normal mice at 1 and 2 h post-injection. In brief, [^{99m}Tc]Tc-HYNIC-ALUG (50 µL, 7.4×10^7 Bq) was injected via tail vein and animals were dissected after 1 and 2 h post injection. The interested tissues and organs were removed, weighed, and counted on γ-counter and the percentage injected dose per gram (%ID/g) was calculated.

Clinical studies of [^{99m}Tc]Tc-HYNIC-ALUG

Clinical test cases [^{99m}Tc]Tc-HYNIC-ALUG performed at Karachi Institute of Radiotherapy and Nuclear Medicine (KIRAN, Karachi) after approval from institutional ethical committee. Patients were explained the procedure and they gave written consent. Whole-body imaging was carried out as per institutional protocol after 7.4×10^4 Bq - 1.11×10^9 Bq radiopharmaceutical injection. Subsequently whole body planar and SPECT-CT imaging from base of skull to the pelvis were carried out in two patients. Areas of abnormal tracer uptake consistent with PSMA expressing lesions were determined and recorded. Image analysis and interpretation were done by two nuclear physicians independently. Areas of disagreement were resolved by consensus [24].

RESULTS AND DISCUSSION

In silico studies

Docking simulation predicts that HYNIC-ALUG has interactions within the active pocket S1' of GCPII is defined by residues Phe 209, Arg 210 and Tyr 700. The putative residues of the S1 pocket Ser 454, Gly 548, Tyr 549 and Tyr 552, as well as with two arginine residues Arg 463 and Arg 536 interact with the ligand. It also binds one of the carboxylates of Asp 387 involved in coordination with two zinc ions located in the rhGCPII active site. Residues of the GCPII receptor also form hydrogen bonding with TYR 234, ARG 536 and ARG 210, also exhibit nonbonding interactions with ARG 534, LYS 207 and GLN 254 which can be seen in Figures 1 and 2.

The calculated LogP and LogS values of HYNIC-ALUG predict its excellent distribution in biological fluids. The LogP value is less than 5, while the LogS, polar surface area (PSA) and relative PSA are also comparable to marketed drugs and very close to the required parameters for a drug candidate. Furthermore, the experimental LogP (–2.69 ± 0.13) is close to the calculated values (miLogP –4.04 and cLogS –3.07), also supporting the validity of in silico studies. Toxicity risk calculations also predict that it has no mutagenic, irritating, or reproductive toxicities except tumorigenic. Evaluation of molecular complexity and flexibility score shows that it does not have a very complex structure, which can also be synthesized in the laboratory to meet its demand (Table 1). PSMA quantitative structure-activity relationship (QSAR) calculations were performed and the HOMO and LUMO energy gap was found 0.1173 eV dipole moment 9.379 Debye and molecular optimization energy -1997.39 as shown in Figure 3.

Preparation of kit and radiolabeling [^{99m}Tc]Tc-HYNIC-ALUG

HYNIC is one of the most commonly used bifunctional chelators for labeling of biomolecules with ^{99m}Tc. However, HYNIC cannot fulfill the coordination number of ^{99m}Tc, coligand is used to complete the coordination sphere [25]. These coligand play important role in radiolabeling, stability, hydrophilicity, pharmacokinetic, tumor uptake and clearance of radiotracers from non-targeted tissues [26]. The coligands often utilized for [^{99m}Tc]Tc-HYNIC conjugates are EDDA/tricine and TPPS/tricine [27]. EDDA/tricine coligand is frequently utilized for radiolabeling of peptides, including RGD, somatostatin, and bombesin. The results of these studies demonstrated significant tumor uptake, quick renal excretion, low activity in blood, and reduced activity in the abdominal area [28-30]. In line with previous studies, for this work, EDDA/tricine was selected as the coligands to obtain [^{99m}Tc]Tc-HYNIC-ALUG in high radiochemical purity [11]. D-Mannitol is broadly used as a bulking agent and filler, and was included in the formulation of the HYNIC-ALUG kit to facilitate efficient freeze-drying and to improve the appearance of the freeze-dried kit. The use of D-Mannitol resulted in the formation of a porous pellet compared to the formulation without it, thus it was included in the final HYNIC-ALUG kit preparation. [^{99m}Tc]Tc-HYNIC-ALUG was prepared by adding sterile Na[$^{99m}TcO_4$] (1 mL, 7.4 $\times 10^4$ Bq-1.11$\times 10^9$ Bq) to HYNIC-ALUG (Figure 4). All quality control parameters are shown in (Table 2). Radio-HPLC analysis also showed that there was no obvious decomposition product, which means that the complex had excellent stability in vitro. The radiochemical purity was assessed by ITLC-SG using two solvent systems, methyl ethyl ketone (MEK) and 0.1 M sodium citrate (Figure 5a, 5b). The radiochemical purity was ($\geq$ 99.1 ± 1.32 %) (Figure 6).

Stability study in serum and determination of partition coefficient

The invitro stability of [^{99m}Tc]Tc-HYNIC-ALUG was assessed in serum, demonstrating excellent stability after 4 h with $\geq$ 95% of [^{99m}Tc] Tc-HYNIC-ALUG remained intact. To determine partition

coefficient, [^{99m}Tc]Tc-HYNIC-ALUG was partitioning in octanol and PBS, yielding a value -2.69 ± 0.137. This value indicated the hydrophilic nature of the complex which is in good agreement with other [^{99m}Tc]Tc-PSMA radiotracer reported in the literature indicating that [^{99m}Tc]Tc-HYNIC-ALUG showed similar characteristic in vivo [31].

In vivo studies in mice

The highest uptake was observed in kidney (31.99 ±0.32 % ID/g) and (13.14 ± 0.44 %ID/g) at 1 h and 2 h post injection respectively (Table 3), which can be related to the physiological PSMA expression in the kidneys and is compatible with the other radiolabeled compounds of PSMA e.g., [^{188}Re]Re-HYNIC-PSMA, [^{177}Lu]Lu-PSMA-617, [^{68}Ga]Ga-PSMA-617 and [^{99m}Tc]Tc-HYNIC-ALUG [6, 32, 33].The biodistribution profile of radiolabeled peptide is significantly influenced by the chelating system and coligands. A radiocomplex with high hydrophilicity has poor protein binding, lower uptake in abdominal region, and high renal excretion [34]. Second highest uptake was observed in blood and spleen was 2.76 ±1.23 and 2.39 ± 1.27 respectively, and another reason for high kidney uptake is the hydrophilic nature of [^{99m}Tc]Tc-HYNIC-PSMA, which makes the kidney the primary excretion pathway. Regarding clinical translation, the expression of PSMA in the kidneys of mice is higher than expression levels in human kidneys [35]. Tubular reabsorption, which is influenced by the electrostatic interaction between the cationic component of the peptides and the negative charge surface of the proximal tubule cells, is one of the mechanisms that might alter the retention period of radioligands in the kidneys. Low kidney retention after 1 h (post injection) led to desired imaging of abdominal tumors like prostate carcinoma.

Clinical studies of [^{99m}Tc]Tc-HYNIC-PSMA

In the two test cases of the prostate (PCa), [^{99m}Tc]Tc-HYNIC-ALUG was injected and imaging was done after 3 hours. Any localized uptake of PSMA that was greater than the surrounding background and did not correspond with physiological tracer uptake was assessed visually as suggesting malignancy.

The first patient (Figure 7) aged 65 years was newly diagnosed with prostate cancer having raised PSA levels. Scan revealed physiologic PSMA uptake in lacrimal and salivary glands, liver, kidneys and urinary bladder. Prostate was slightly enlarged in size with PSMA avid area. Furthermore, foci of abnormal tracer uptake were noted in the skull (right parietal bone), left 8th rib, lymph nodes (mediastinum, abdomen and pelvis) and right iliac bone. The patient aged was 72 years on bisphosphonates and anti-androgens for 2 years with recent increase in PSA levels (Figure 8). Scan showed PSMA uptake in lacrimal and salivary glands, liver, kidneys and urinary bladder. PSMA uptake also noted in enlarged prostate, osseous and nodal metastasis. Clinical results found to be comparable with the work reported in literature. Our results also indicated that PSA kinetics affected the sensitivity of [^{99m}Tc]Tc-HYNIC-PSMA SPECT/CT. The PSA levels and kinetics were beneficial for selecting patients who would likely benefit from SPECT/CT imaging. This agent may significantly improve the diagnosis, staging, and subsequent monitoring of therapeutic effects in PCa patients.

CONCLUSION

[^{99m}Tc]Tc-HYNIC-ALUG kit was successfully prepared and efficiently labeled with ^{99m}Tc with radiochemical efficiency ≥ 99 % after incubation for 15 min in boiling water bath. It exhibited high stability in human serum even after 4 h, with ≥ 95% ^{99m}Tc remain intact with HYNIC-ALUG. The hydrophilic nature of the [^{99m}Tc]Tc-HYNIC-ALUG, (Log P =-2.69), suggests fast elimination

through the kidneys and other non-targeted tissues. The results demonstrated the specific accumulation of [^{99m}Tc]Tc-HYNIC-ALUG in PSMA-positive tumors and low background levels in other organs. This study confirmed previous reports that [^{99m}Tc]Tc-HYNIC-ALUG SPECT/CT has great potential as an imaging modality in the evaluation of recurrent PCa patients after RP. The present investigation has certain constraints. Late imaging was not feasible and the follow-up duration was relatively short. However, it is anticipated that this kit formulation will address previous limitations of ^{99m}Tc-based PSMA conjugates. Additionally, larger trials are essential to elucidate its potential in the management of PCa.

REFERENCES

1. Osdzich P, Darr C, Hilser T, Wahl M, Herrmann K, Hadaschik B, Grünwald V. Metastatic prostate cancer-a review of current treatment options and promising new approaches. Cancers (Basel). 2023 Jan 11;15(2):461.
2. Xia C, Dong X, Li H, Cao M, Sun D, He S, Yang F, Yan X, Zhang S, Li N, Chen W. Cancer statistics in China and United States, 2022: profiles, trends, and determinants. Chin Med J (Engl). 2022 Feb 9;135(5):584-90.
3. Center MM, Jemal A, Lortet-Tieulent J, Ward E, Ferlay J, Brawley O, Bray F. International variation in prostate cancer incidence and mortality rates. Eur Urol. 2012 Jun;61(6):1079-92.
4. Maurer T, Eiber M, Schwaiger M, Gschwend JE. Current use of PSMA-PET in prostate cancer management. Nat Rev Urol. 2016 Apr;13(4):226-35.
5. Bryant RJ, Hamdy FC. Screening for prostate cancer: an update. Eur Urol. 2008 Jan;53(1):37-44.
6. Sharifi M, Yousefnia H, Bahrami-Samani A, Jalilian AR, Zolghadri S, Vaez-Tehrani M, Maus S. Optimized production assessment, compartmental modeling and dosimetric evaluation of 177Lu-PSMA-617 for clinical trials. Int J Nucl Med Res. 2017;4:45-52.
7. Santoni M, Scarpelli M, Mazzucchelli R, Lopez-Beltran A, Cheng L, Cascinu S, Montironi R. Targeting prostate-specific membrane antigen for personalized therapies in prostate cancer: morphologic and molecular backgrounds and future promises. J Biol Regul Homeost Agents. 2014 Oct-Dec;28(4):555-63.
8. Brunello S, Salvarese N, Carpanese D, Gobbi C, Melendez-Alafort L, Bolzati C. A review on the current state and future perspectives of [99mTc] Tc-housed PSMA-i in prostate cancer. Molecules. 2022;27:2617.
9. Ferro-Flores G, Luna-Gutiérrez M, Ocampo-García B, Santos-Cuevas C, Azorín-Vega E, Jiménez-Mancilla N, Orocio-Rodríguez E, Davanzo J, García-Pérez FO. Clinical translation of a PSMA inhibitor for ^{99m}Tc-based SPECT. Nucl Med Biol. 2017 May;48:36-44.
10. Garnuszek P, Karczmarczyk U, Maurin M, Sikora A, Zaborniak J, Pijarowska-Kruszyna J, Jaroń A, Wyczółkowska M, Wojdowska W, Pawlak D, Lipiński PFJ, Mikołajczak R. PSMA-D4 radioligand for targeted therapy of prostate cancer: synthesis, characteristics and preliminary assessment of biological properties. Int J Mol Sci. 2021 Mar 8;22(5):2731.
11. Xu X, Zhang J, Hu S, He S, Bao X, Ma G, Luo J, Cheng J, Zhang Y. ^{99m}Tc-labeling and evaluation of a HYNIC modified small-molecular inhibitor of prostate-specific membrane antigen. Nucl Med Biol. 2017 May;48:69-75.

12. Werner RA, Derlin T, Lapa C, Sheikbahaei S, Higuchi T, Giesel FL, Behr S, Drzezga A, Kimura H, Buck AK, Bengel FM, Pomper MG, Gorin MA, Rowe SP. ^{18}F-Labeled, PSMA-targeted radiotracers: leveraging the advantages of radiofluorination for prostate cancer molecular imaging. Theranostics. 2020 Jan 1;10(1):1-16.

13. Jacobson O, Kiesewetter DO, Chen X. Fluorine-18 radiochemistry, labeling strategies and synthetic routes. Bioconjug Chem. 2015 Jan 21;26(1):1-18.

14. Fendler WP, Calais J, Eiber M, Flavell RR, Mishoe A, Feng FY, Nguyen HG, Reiter RE, Rettig MB, Okamoto S, Emmett L, Zacho HD, Ilhan H, Wetter A, Rischpler C, Schoder H, Burger IA, Gartmann J, Smith R, Small EJ, Slavik R, Carroll PR, Herrmann K, Czernin J, Hope TA. Assessment of 68Ga-PSMA-11 PET accuracy in localizing recurrent prostate cancer: a prospective single-arm clinical trial. JAMA Oncol. 2019 Jun 1;5(6):856-63.

15. Lawal IO, Ankrah AO, Mokgoro NP, Vorster M, Maes A, Sathekge MM. Diagnostic sensitivity of Tc-99m HYNIC PSMA SPECT/CT in prostate carcinoma: A comparative analysis with Ga-68 PSMA PET/CT. Prostate. 2017 Aug;77(11):1205-12.

16. Boschi A, Uccelli L, Martini P. A picture of modern Tc-99m radiopharmaceuticals: Production, chemistry, and applications in molecular imaging. Appl Sci. 2019(12);9:2526.

17. Rezazadeh F, Sadeghzadeh N. Tumor targeting with ^{99m} Tc radiolabeled peptides: Clinical application and recent development. Chem Biol Drug Des. 2019 Mar;93(3):205-21.

18. Lebowitz E, Richards P. Radionuclide generator systems. Semin Nucl Med. 1974 Jul;4(3):257-68.

19. Nairne J, Iveson PB, Meijer A. Imaging in drug development. Prog Med Chem. 2015;54:231-80.

20. Urbán S, Meyer C, Dahlbom M, Farkas I, Sipka G, Besenyi Z, Czernin J, Calais J, Pávics L. Radiation dosimetry of ^{99m}Tc-PSMA I&S: a single-center prospective study. J Nucl Med. 2021 Aug 1;62(8):1075-81.

21. Kim MH, Kim SG, Kim DW. Dual-labeled prostate-specific membrane antigen (PSMA)-targeting agent for preoperative molecular imaging and fluorescence-guided surgery for prostate cancer. J Labelled Comp Radiopharm. 2021 Jan;64(1):4-13.

22. Rathke H, Afshar-Oromieh A, Giesel FL, Kremer C, Flechsig P, Haufe S, Mier W, Holland-Letz T, De Bucourt M, Armor T, Babich JW, Haberkorn U, Kratochwil C. Intraindividual comparison of ^{99m}Tc-methylene diphosphonate and prostate-specific membrane antigen ligand ^{99m}tc-mip-1427 in patients with osseous metastasized prostate cancer. J Nucl Med. 2018 Sep;59(9):1373-9.

23. Torre LA, Bray F, Siegel RL, Ferlay J, Lortet-Tieulent J, Jemal A. Global cancer statistics, 2012. CA Cancer J Clin. 2015 Mar;65(2):87-108.

24. Liu C, Zhu Y, Su H, Xu X, Zhang Y, Ye D, Hu S. Relationship between PSA kinetics and Tc-99m HYNIC PSMA SPECT/CT detection rates of biochemical recurrence in patients with prostate cancer after radical prostatectomy. Prostate. 2018 Dec;78(16):1215-21.

25. Decristoforo C, Mather SJ. The influence of chelator on the pharmacokinetics of 99mTc-labelled peptides. Q J Nucl Med. 2002 Sep;46(3):195-205.

26. Shaghaghi Z, Abedi SM, Hosseinimehr SJ. Tricine co-ligand improved the efficacy of ^{99m}Tc-HYNIC-$(Ser)_3$-J18 peptide for targeting and imaging of non-small-cell lung cancer. Biomed Pharmacother. 2018 Aug;104:325-31.

27. Maurer T, Eiber M, Schwaiger M, Gschwend JE. Current use of PSMA-PET in prostate cancer management. Nat Rev Urol. 2016 Apr;13(4):226-35.

28. Decristoforo C, Mather SJ. 99m-Technetium-labelled peptide-HYNIC conjugates: effects of lipophilicity and stability on biodistribution. Nucl Med Biol. 1999 May;26(4):389-96.

29. Hubalewska-Dydejczyk A, Fröss-Baron K, Mikołajczak R, Maecke HR, Huszno B, Pach D, Sowa-Staszczak A, Janota B, Szybiński P, Kulig J. 99mTc-EDDA/HYNIC-octreotate scintigraphy, an efficient method for the detection and staging of carcinoid tumours: results of 3 years' experience. Eur J Nucl Med Mol Imaging. 2006 Oct;33(10):1123-33.

30. King R, Surfraz MB, Finucane C, Biagini SC, Blower PJ, Mather SJ. 99mTc-HYNIC-gastrin peptides: assisted coordination of 99mtc by amino acid side chains results in improved performance both In Vitro and In Vivo. J Nucl Med. 2009 Apr;50(4):591-8.

31. Xu X, Zhang J, Hu S, He S, Bao X, Ma G, Luo J, Cheng J, Zhang Y. ^{99m}Tc-labeling and evaluation of a HYNIC modified small-molecular inhibitor of prostate-specific membrane antigen. Nucl Med Biol. 2017 May;48:69-75.

32. Hadisi M, Vosoughi N, Yousefnia H, Bahrami-Samani A, Zolghadri S, Vosoughi S, Alirezapour B. Preclinical evaluation of 188 Re-HYNIC-PSMA as a novel therapeutic agent. J Radioanal Nucl Chem. 2022;2:841-9.

33. Sharifi M, Yousefnia H, Zolghadri S, Bahrami-Samani A, Naderi M, Jalilian AR, Geramifar P, Beiki D. Preparation and biodistribution assessment of 68 Ga-DKFZ-PSMA-617 for PET prostate cancer imaging. Nucl Sci Tech. 2016;27(6):1-9.

34. Masteri Farahani A, Maleki F, Sadeghzadeh N, Abediankenari S, Abedi SM, Erfani M. ^{99m} Tc-(EDDA/tricine)-HYNIC-GnRH analogue as a potential imaging probe for diagnosis of prostate cancer. Chem Biol Drug Des. 2020 Aug;96(2):850-60.

35. Lodhi NA, Park JY, Kim K, Hong MK, Kim YJ, Lee Y-S, Cheon GJ, Kang KW, Jeong JM. Synthesis and evaluation of 99mTc-tricabonyl labeled isonitrile conjugates for prostate-specific membrane antigen (PSMA) Image. Inorganics. 2020; 8(1):5.

Table 1. In silico Calculations and Molecular Modeling Data for HYNIC-ALUG, PSMA

Molinspiration Bioactivity		**Data Warrior Calculations**				**Docking Score of HYNIC-ALUG, PSMA**	
Bioactivity	Score/value	Property	Value	Toxicity & Molecular Structure	Prediction	Docked Ligand parameters	Docking Score
GPCR ligand	0.12	cLogP	0.0997	Mutagenic	none	Binding energy	-7.29
Ion channel modulator	-0.37	cLogS	-3.069	Tumorigenic	High	Ki (µM)	4.55
Kinase inhibitor	-0.15	H-Acceptors	16	Reproductive effective	None	Intermolecular energy	-14.45
Nuclear receptor ligand	-0.44	H-Donors	9	Irritant	None	Internal energy	-1.42
Protease inhibitor	0.23	Total surface area	439.75	Nasty functions	hydrazine	Tortional energy	7.16
Enzyme inhibitor	0.1	Relative PSA	0.45726	Shape Index	0.7	Unbound extended energy	-1.42
Blood brain barrier	0.874	Polar surface area	262.17	Molecular Flexibility	0.61618	Ref RMS	61.46
Plasma protein binding	42.439	Drug likeness	-20.559	Molecular complexity	0.7177	Volume	509.62

Table 2. Quality control parameters for [^{99m}Tc] Tc-HYNIC-PSMA

Test	**Appearance criteria**	**Procedures**
Appearance	Colorless liquid, free from any particulate matter	Visualization in adequate light
pH	6-7	pH paper
Radiochemical purity	>99% retention time and peak area.	ITLC-SG/Radio-HPLC
Sterility test	Sterile as per PP	Pakistani pharmacopoeia procedures
Bacterial endotoxin test (BET)	Negative	Pakistani pharmacopoeia procedures

Table 3. Biodistribution studies of [^{99m}Tc]Tc-HYNIC-ALUG in normal mice

Organs	**Mean %ID/g (1h p.i.)**	**Mean %ID/g (2h p.i.)**
Liver	2.20 ± 0.76	1.06 ±0.92
Spleen	0.68 ±0.12	1.97 ±0.56
Stomach	0.55 ±0.33	0.18 ±0.02
Intestine	4.69 ±3.76	1.04 ±0.46
Lungs	0.95 ±0.18	0.85 ±0.30
Kidneys	31.99 ±0.32	13.14 ±0.44
Femur	1.60 ±0.09	0.61 ±0.12
Bladder	3.76 ±3.52	0.28 ±0.03
Heart	1.54 ±0.12	0.97 ±0.01

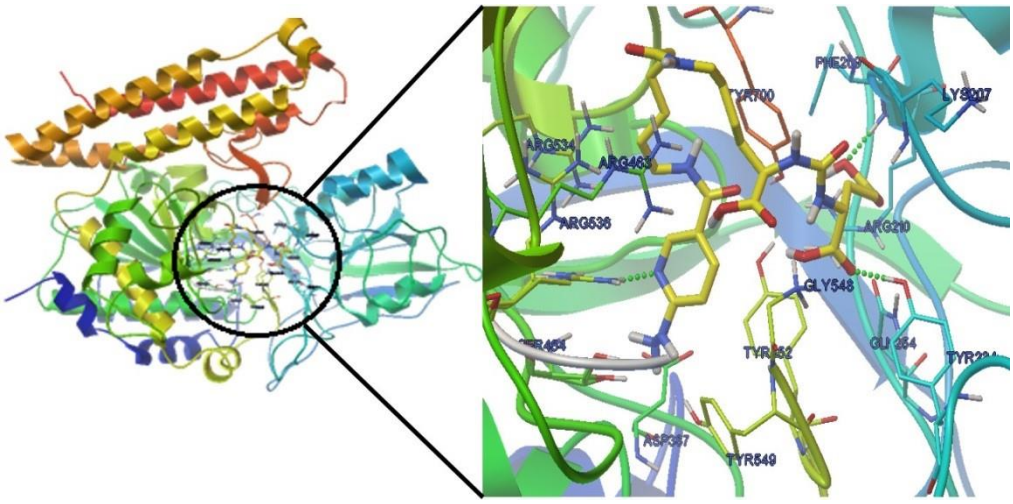

Fig 1. PSMA precursor interactions within the active pocket **S1** of GCPII (PDB ID 2OOT)

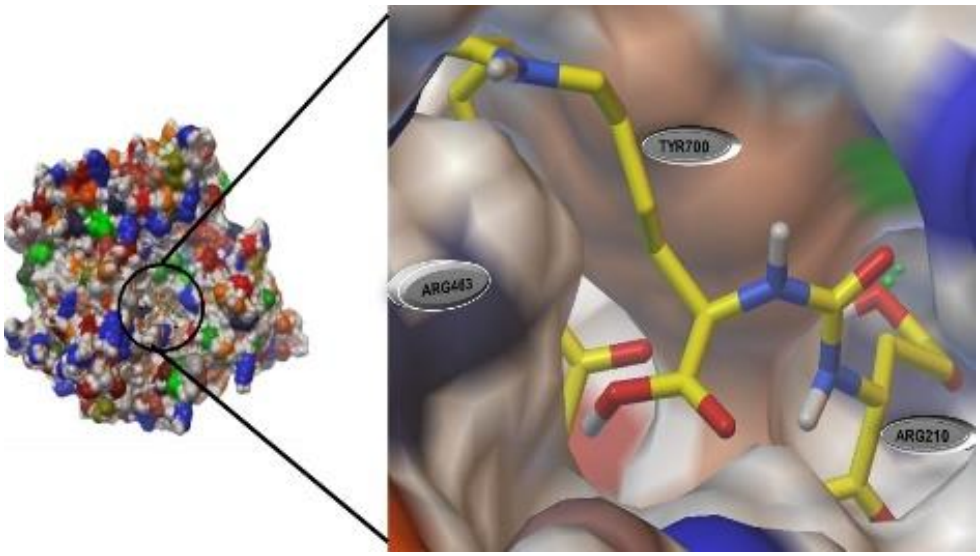

Fig 2. MMS view of PSMA precursor within the active pocket S1 of GCPII (PDB ID 2OOT)

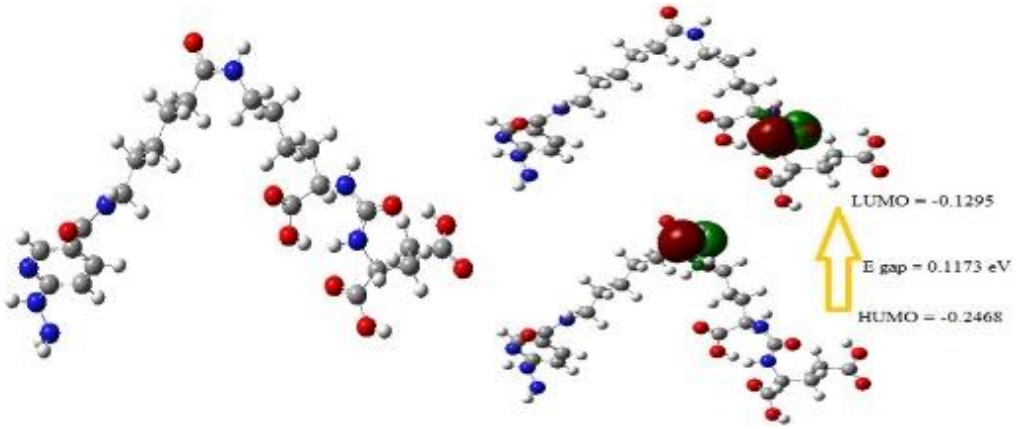

Fig 3. 3D Gaussian optimized structure of HYNIC-ALUG, PSMA along with HUMO and LUMO energy gap

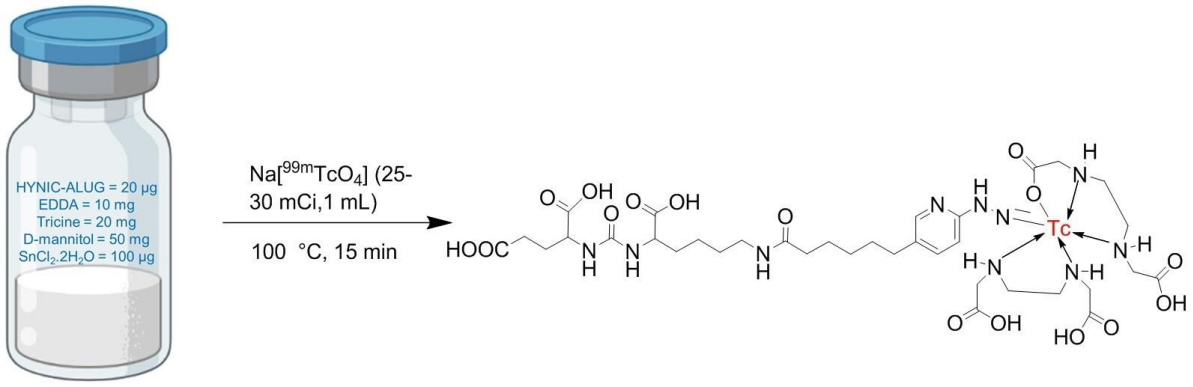

Fig 4. Structure of [^{99m}Tc]Tc-HYNIC-ALUG

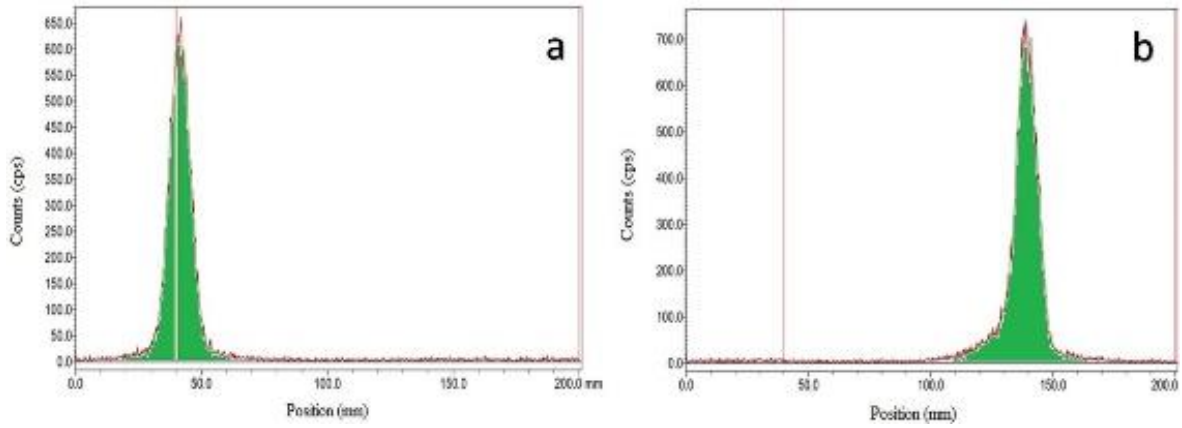

Fig 5. **(a)** ITLC-SG chromatogram showing RCP of [^{99m}Tc]Tc-HYNIC-ALUG in MEK solvent, **(b)** ITLC-SG chromatogram showing RCP of [^{99m}Tc]Tc-HYNIC-ALUG in solvent TSC

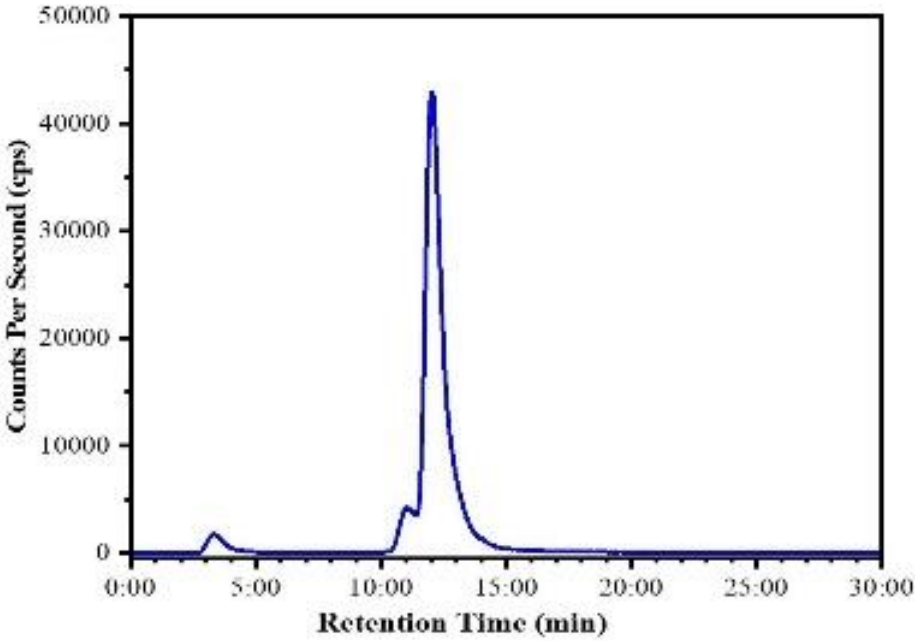

Fig 6. Radio-HPLC of [^{99m}Tc]Tc-HYNIC-ALUG in 0.1%TFA water and 0.1% TFA in acetonitrile using gradient elution

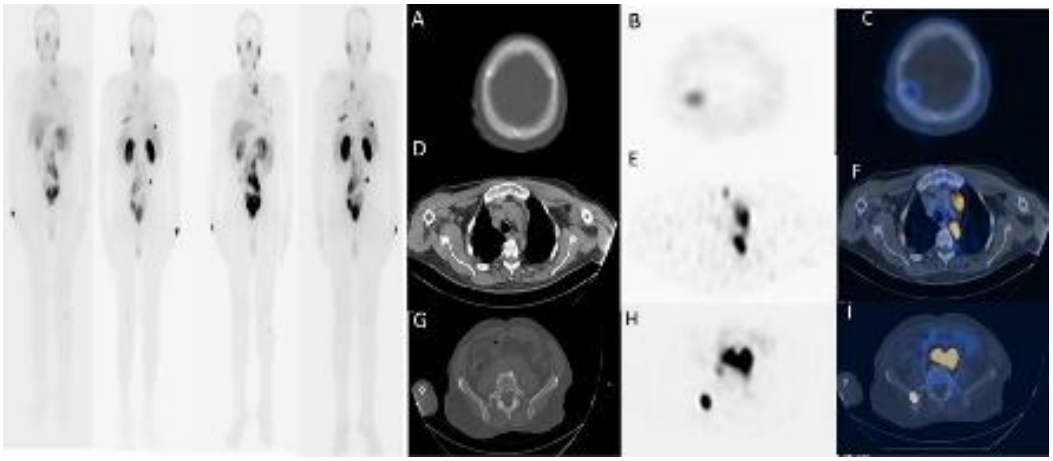

Fig 7. Whole body PSMA planar imaging showing physiologic PSMA uptake along with abnormal foci of tracer uptake in the skull, upper chest, left 8th rib posteriorly, abdomen and pelvis. A, B and C are SPECT/CT images of radiotracer uptake in right parietal bone. D, E and F are SPET/CT images of radiotracer uptake in left mediastinal lymph node. G, H and I are SPET/CT images of radiotracer uptake in right ilium near right sacro-iliac joint, respectively

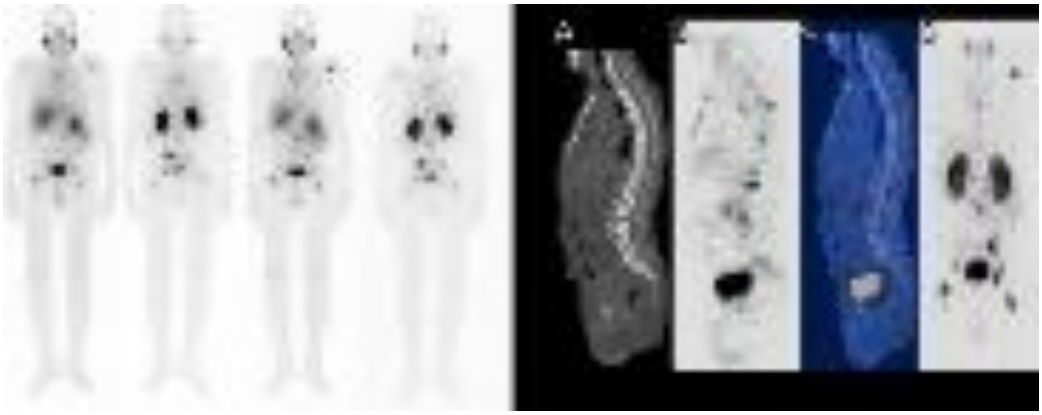

Fig 8. Whole body planar imaging of PSMA uptake showing abnormal foci of tracer uptake in the chest, liver and bones in patient having Ca Prostate with bony metastasis, on Zometa since December, 2020. A, B, C & D are the SPECT/CT images of PSMA uptake in multiple vertebra metastasis.